



Adsorption of Eosin Y using an environmentally friendly adsorbent prepared by microwave heating

Jianhua Shu^{a,b,c,d}, Hongying Xia^{a,b,c,d,*}, Libo Zhang^{a,b,c,d}, Jinhui Peng^{a,b,c,d},
Song Cheng^{a,b,c,d}, Chunyang Li^{a,b,c,d}

^aYunnan Provincial Key Laboratory of Intensification Metallurgy, Kunming University of Science and Technology, Kunming, Yunnan 650093, China, emails: hyxia@kmust.edu.cn (H. Xia), 1412076790@qq.com (J. Shu), libozhang77@163.com (L. Zhang), jhpeng@kmust.edu.cn (J. Peng), 18388402089@163.com (S. Cheng), 1391362943@qq.com (C. Li)

^bState Key Laboratory of Complex Nonferrous Metal Resources Clean Utilization, Kunming University of Science and Technology, Kunming, Yunnan 650093, China

^cNational Local Joint Laboratory of Engineering Application of Microwave Energy and Equipment Technology, Kunming, Yunnan 650093, China

^dFaculty of Metallurgical and Energy Engineering, Kunming University of Science and Technology, Kunming, Yunnan 650093, China

Received 23 August 2017; Accepted 10 February 2018

ABSTRACT

Eosin Y is a kind of organic dye which is difficult to degrade, and it has a harmful effect on water quality. In this work, the removal efficiency of Eosin Y from aqueous solutions by the spent activated carbon (AC) which is regenerated via microwave heating has been systematically investigated. The structure and properties of spent AC and regenerated AC were characterized by N₂ adsorption isotherms, scanning electron microscopy, Fourier-transform infrared spectroscopy, X-ray photoelectron spectroscopy and gas chromatography-mass spectrometry. The related dominant factors including contact time, pH, temperature, initial concentration and ionic strength were considered, and these effects on the removal of Eosin Y were studied in batch experiments. Additionally, based on the best fit rule, kinetic and isotherm studies indicated that the experimental data were in line with the theoretical values predicted by the pseudo-second-order model and the Langmuir adsorption isotherm model, respectively. The maximum adsorption capacity of Eosin Y was 344.83 mg/g, indicating high efficiency for Eosin Y adsorption. Thermodynamic parameters revealed the endothermic nature of the adsorption process. All the present studies showed that using regenerated AC to remove Eosin Y from wastewater is an environmentally friendly way, and the comprehensive utilization of waste resources is also realized.

Keywords: Activated carbon; Adsorption; Eosin Y; GC-MS; Dye

1. Introduction

Organic dyes are widely used in dyestuff, food, papermaking and textile industry. A large amount of toxic, bioaccumulative and organic wastewater is produced in these industries, which can heavily pollute the environment due to their high toxicity and carcinogenic aspects [1–3]. Moreover,

an organic dye containing effluent can increase biochemical oxygen demand. Furthermore, its influences for the ecosystem depend on their concentration, but colored effluents are also evident even in small concentration that seriously affects the water quality and damage the aquatic system [4]. Eosin Y is a kind of organic dye that is difficult to degrade, and it is mainly adopted for indicator adsorption of red ink production and wool dyeing. These processes will produce some pollutants. Besides, these streams of pollutants discharged to the ecological system without any proper treatment will

* Corresponding author.

cause irreparable damage to the environment. Additionally, organic dyes are difficult to be removed due to their high stability against chemical, light and microbial attacks [5–7]. Thus, it is important to find an environmentally friendly and efficient technique to remove organic dyes from wastewater.

Approaches to removing organic pollutants include filtration, adsorption, advanced oxidation processes, ion-exchange and biological treatment [8–11]. The adsorption method is significantly popular in the removal of these pollutants because of its advantages, such as simple, easy operation and strong regeneration capacity [12]. There are several adsorbents available for removing Eosin dye, such as activated carbon (AC), nano-sized chitosan particles [13], chitosan/polyvinyl alcohol (PVA) blend, ethylenediamine, tetraethylenepentamine and biosorbents. AC is one of the commonest adsorbents due to its high porosity, huge surface area and complex internal structure [14]. In addition, AC could be prepared from agricultural residues, coal, oil, plastic, etc. [15,16]. However, it will produce a large number of spent AC after dye wastewater treatment with AC, which is a waste of resources and may pollute the environment. Consequently, it is an effective way to utilize the resources and reduce the environmental pressure through the regeneration of AC via microwave heating [17].

Recently, regenerating spent AC using the microwave heating method has been mentioned in literature. Compared with conventional thermal regeneration, the microwave heating method is featured with some advantages, such as rapid and precise temperature control, possible time, energy savings and no thermal inertia [18]. Microwave material is heated by dielectric, and the heating rate of material is affected by the dielectric constant, while conventional heating is heated by conduction or convection. Moreover, microwave heating can enhance regeneration efficiency, since AC is heated by internal heating, and energy directly penetrates into the AC and generates heat through high frequency internal dipole rotation [19]. Thus, the pollutant adsorbed on the surface of AC was removed easily. Furthermore, some researchers mentioned that regeneration of AC via the microwave heating method can make new pore structures and increase the surface area [20,21].

This research aims to investigate the ability of regenerated AC to remove Eosin Y from aqueous solutions. Spent AC was obtained from production of aspirin, and it was regenerated by microwave heating. This work also discussed the influence of contact time, initial concentration, pH, temperature and ionic strength on the efficiency of the adsorption process. Adsorption mechanisms have been analyzed and discussed through the isotherm, kinetic and thermodynamic studies. In present study, it is rarely reported in literature that regenerated AC was adopted as the adsorbent to remove eosin dye, which was generated from spent AC by microwave heating.

2. Materials and methods

2.1. Materials

Spent AC was obtained from a pharmaceutical company in China. All chemicals used in this research were analytical grade. NaCl ($\geq 99.5\%$), HCl (37%) and NaOH ($\geq 99.5\%$) were purchased from a chemical company in Tianjin, China.

Eosin Y (empirical formula $C_{20}H_6Br_4Na_2O$) is an organic dye employed in the adsorption of indicators, the production of red inks and wool dyeing.

2.2. Activated carbon regeneration

Spent AC was obtained from the production of aspirin, and it was dried in a laboratory at 105°C for 12 h to remove moisture. Then, 8 g spent AC was placed into the ceramic crucible each time to carry out a series of experiments in a box type microwave oven. Besides, the single factor method was adopted to study the effects of regeneration temperature (500°C – 900°C), regeneration time (5–10 min) and material thickness (15–25 cm) on the adsorption properties of AC. With the increase of regeneration temperature, regeneration time and material thickness, adsorption capacity of regenerated AC increased at first and then decreased. Therefore, the optimal conditions obtained from experiments are regeneration temperature of 700°C , regeneration time of 10 min and material thickness of 20 mm. Under these conditions, AC with larger surface area was obtained, and it was used for adsorption experiments and characterization.

2.3. Characterization of activated carbon

AC was characterized by the following various techniques. The pore properties of AC were featured with an Autosorb-1 physical and chemical adsorption instrument of N_2 at 77 K (Quantachrome Instruments Trading Company Limited, USA). The surface texture and morphology of the samples were observed with a scanning electron microscope (SEM; Philips XL30ESEM-TMP, USA). Fourier-transform infrared spectroscopy (FTIR; Nicoletis10, Thermo Fisher Scientific, USA) was obtained between 4,000 and 400 cm^{-1} . X-ray photoelectron spectroscopy (XPS) was performed on a PHI 5500 electron spectrometer (Physical Electronics, Inc., Chanhassen, MN, USA) with 200 W Mg radiations. Gas chromatography-mass spectrometry (GC-MS; Thermo, Trace 1310-ISQ LT, USA) was used to identify the organic compounds in the solution at the He and column flow rate of 1 mL/min. A TG-5 column ($30\text{ m} \times 0.25\text{ }\mu\text{m} \times 0.25\text{ mm}$) was used in GC-MS. An oven program was set at 50°C for 2 min and then it was raised to 200°C with a heating rate of $5^\circ\text{C}/\text{min}$. Finally, it was raised to 300°C at $10^\circ\text{C}/\text{min}$. The injected volume was 1 μL with a split mode.

2.4. Batch studies and analysis methods

Adsorption experiments were conducted to verify the extent of removing Eosin Y from organic dye wastewater and adsorption mechanisms. All adsorption experiments were performed at 50 mL centrifuge tubes. Then, 30 mg regeneration of AC was added in 30 mL Eosin Y solution with a certain concentration (100–180 mg/L), and placed in a constant temperature oscillation apparatus with the shaking speed of 345 rpm. The equilibrium isotherms of Eosin Y adsorption were carried out at different temperatures of 20°C , 30°C and 40°C . Eosin Y concentration after adsorption was determined by a visible range spectrophotometer at 524 nm and a standard curve of absorbance vs. concentration. The amount of Eosin Y adsorbed per unit of regeneration of AC

at equilibrium and the removal rate of Eosin Y in the solution were calculated by the following equations:

$$Q_e = [(C_0 - C_e)V]/M \quad (1)$$

$$\text{Removal rate (\%)} = [(C_0 - C_e)/C_0] \times 100\% \quad (2)$$

where C_0 (mg/L) and C_e (mg/L) are the initial and equilibrium concentration of Eosin Y, respectively. V (L) is the volume of a solution and M (g) is the mass of the adsorbent. Q_e (mg/g) represents the adsorption capacity of adsorbents.

Two isotherm models (Freundlich and Langmuir) were adopted to fit the equilibrium data. The equations are expressed as follows:

The Langmuir equilibrium adsorption curve equation is expressed as [22]:

$$\frac{1}{Q_e} = \frac{1}{K_a Q_m C_e} + \frac{1}{Q_m} \quad (3)$$

where K_a is the Langmuir equilibrium constant and Q_m is the amount adsorbed of monolayer coverage on the surface.

The Freundlich equilibrium adsorption curve is given as follows [23]:

$$\log Q_e = \log K_f + \frac{1}{n} \log C_e \quad (4)$$

where K_f and $1/n$ are the temperature constant, which can reflect the adsorption capacity and the adsorption intensity, respectively.

Adsorption kinetic studies were carried out in a series of 50 mL centrifuge tubes under the temperature of 30°C. In addition to that, the adsorption method is similar to the previously described one. The amount of Eosin Y adsorbed per unit of regeneration of AC at time t (Q_t) was calculated by the following equation:

$$Q_t = [(C_0 - C_t)V]/M \quad (5)$$

where C_t (mg/L) is the concentration of Eosin Y at a certain time t (min). The adsorption kinetics of Eosin Y were analyzed using different models such as pseudo-first-order and pseudo-second-order kinetics and intra-particle diffusion to select the most suitable model based on the value of the linear regression correlation coefficient (R^2).

The pseudo-first-order equation [24] is expressed as:

$$\log(Q_e - Q_t) = \log(Q_e) - \frac{k_1}{2.303} t \quad (6)$$

where Q_e and Q_t refer to the amount of Eosin Y adsorbed (mg/g) at equilibrium and at time t (min), respectively, and k_1 is the rate constant of the pseudo-first-order model.

The pseudo-second-order equation [25] is expressed as follows:

$$\frac{t}{Q_t} = \frac{1}{k_2 Q_e^2} + \frac{t}{Q_e} \quad (7)$$

where k_2 is the equilibrium rate constant of the pseudo-second-order model.

The intra-particle diffusion model equation is expressed as follows [26]:

$$Q_t = k_3 t^{1/2} + I \quad (8)$$

where k_3 is the intra-particle diffusion rate constant (mg/(g min^{0.5})) and I is the intercept (mg/g).

3. Results and discussion

3.1. Porous structure analysis

The N_2 adsorption–desorption isotherms of spent AC and regenerated AC are shown in Fig. 1, while pore-size distribution curves are presented in Fig. 2. According to the International Union of Pure and Applied Chemistry (IUPAC) classification [27], N_2 adsorption–desorption isotherms

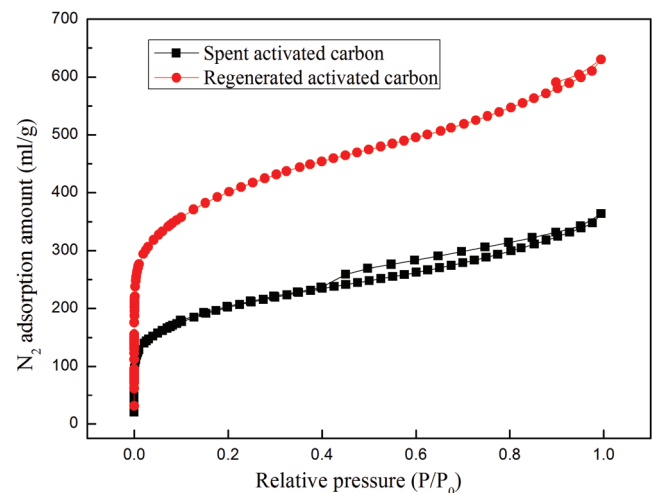


Fig. 1. N_2 adsorption–desorption isotherms of spent activated carbon and regenerated activated carbon.

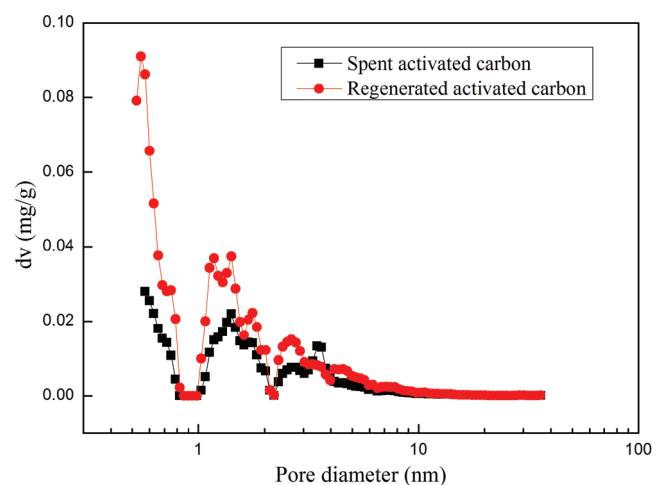


Fig. 2. Pore-size distributions of spent activated carbon and regenerated activated carbon.

presented IV type, and exhibiting characteristics of microporous and mesoporous materials. Besides, the curves of pore-size distribution showed that most pores are distributed between 0 and 35 nm, mainly indicating microporous and mesoporous. The pore structure parameters obtained from the N_2 adsorption–desorption isotherms and pore-size distribution curves are shown in Table 1. Compared with the spent AC, the pore structure parameters of regenerated AC were improved [28]. Nor et al. [29] believed that microwave heating regeneration of spent AC increases the pore volume which influences the increase in the surface area of AC, where high development of micropore volumes is obtained. Therefore, microwave regeneration enhances the properties of spent AC. For example, the Brunauer–Emmett–Teller (BET) surface area is increased by $628 \text{ m}^2/\text{g}$ after regeneration using microwave heating. As can be observed, these two materials show the mesoporous feature, with pore diameters between 2 and 10 nm.

3.2. SEM analysis

Fig. 3 shows SEM images of spent AC (A), regenerated AC (B) and AC after adsorption (C). These images can be employed to verify the possible changes in surface morphology of samples during the experiment process. Obviously, there is a significant difference in surface morphology among these three samples. Fig. 3(A) shows that the surface of spent AC was relatively rough and irregular, and obvious pores cannot be seen on the surface [28]. After microwave heating regeneration (Fig. 3(B)), the surface of AC becomes relatively flat and smooth, and there are a lot of pores that are in favor of adsorption. Besides, the AC after adsorption was shown in Fig. 3(C), indicating that the surface and pores were filled up with a lot of impurities. It can be concluded that regeneration after microwave heating can improve some physical characteristics and adsorption capacity of AC. Compared with Figs. 3(A) and (C), the pores of AC after regeneration adsorbed a large amount of materials which indicated that microwave heating regeneration improves the adsorption capacity of spent AC.

3.3. FTIR and XPS analysis

FTIR was used to examine the mainly functional groups existing in these samples of spent AC, regenerated AC and AC after adsorption of Eosin Y (Fig. 4). These functional groups play significant roles in adsorption of contaminant

Table 1

Pore characteristic parameters of spent activated carbon and regenerated activated carbon

Characteristic	Spent activated carbon	Regenerated activated carbon
BET surface area (m^2/g)	667.8	1,296
Total pore volume (mL/g)	0.5639	0.9774
Average pore size (nm)	3.378	3.016
Micropore volume (mL/g)	0.2179	0.4673
Micropore ratio (%)	38.64	47.81

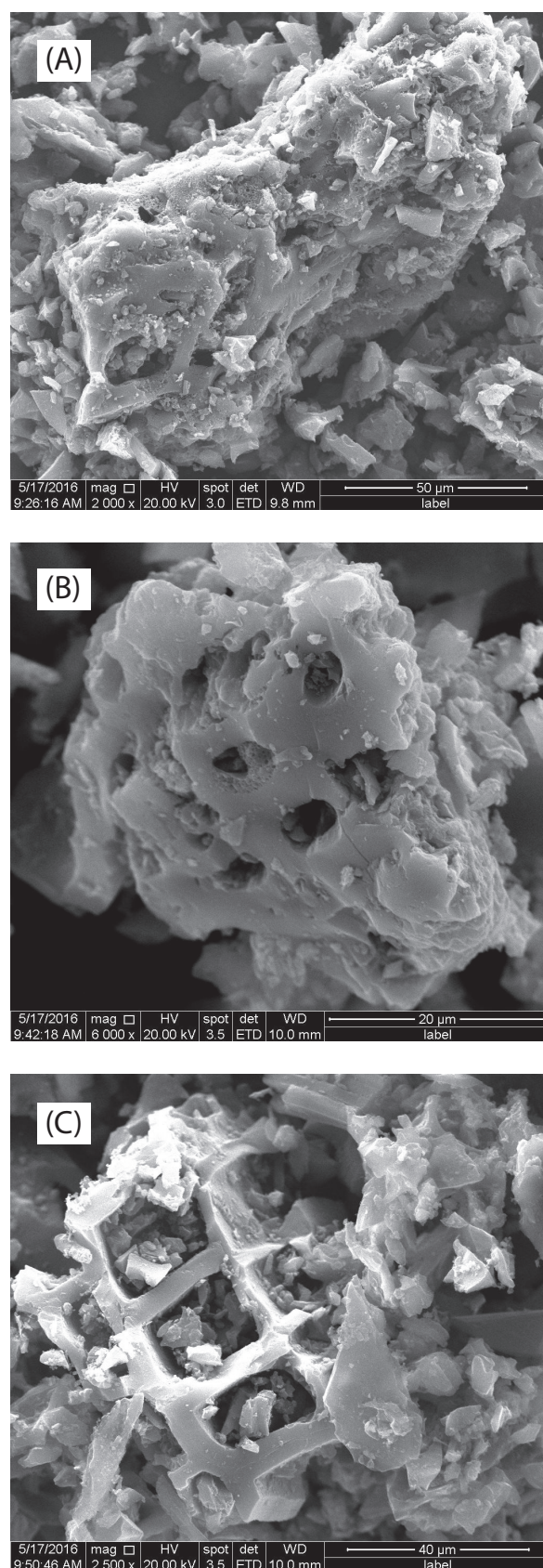


Fig. 3. SEM of spent AC (A), regenerated AC (B) and AC after adsorption (C).

ions [30]. The FTIR of samples was recorded between 4,000 and 400 cm^{-1} . It is obvious that the FTIR is similar, indicating the same functional groups [31]. As shown in Fig. 4, there was a clear high intense peak at 3,428 cm^{-1} of all samples. The peak at 3,428 cm^{-1} can be attributed to O–H and N–H stretching vibration for adsorbed water. The peak around 2,924 cm^{-1}

is corresponding to the stretching vibration of the C–H group and is caused by CO_2 in the air, characteristic of olefins, aliphatic and aromatics. The peak at 1,616 cm^{-1} is attributed to C=O and C=C groups stretching vibration and characteristic of carbonyl compounds. The bands around 1,300–1,500 cm^{-1} can be assigned to C–O, C–H or C–C stretching vibration. The strong adsorption band at 1,114 cm^{-1} is possibly attributed to the C–O group stretching vibration of carboxylate and characteristic of aliphatic ether. The bands between 400 and 900 cm^{-1} may exist in organic halide. Furthermore, some important functional groups were kept in AC, which can play a role in the adsorption process [32].

XPS is a technique that can be employed to characterize the composition and surface groups of materials. The XPS spectra of spent AC and regenerated AC are shown in Figs. 4(B) and (C), respectively. Peaks of the C 1s spectra stem from spent AC and regenerated AC containing many impurities, mainly consisting of carbon, hydrocarbon and carbonyl. As shown in Fig. 4(B), it is suitable for the energy of 284.3 eV (C–C), 285.5 eV (C–O) and 287.9 eV (C=O), respectively. Besides, it is observed in Fig. 4(C) that these impurities suited at the energy of 284.5 eV (C–C), 285.9 eV (C–O) and 289.9 eV (C=O), respectively. Li et al. [33] reported that C–C, C–O and C=C were situated at the energy of 284.20, 285.32 and 287.95 eV. After regeneration, the content of C–O and C=O of AC increases from 21.51% to 23.95% and from 9.65% to 13.85%, which are the main groups of adsorbing Eosin Y.

3.4. GC-MS analysis

GC-MS is an extremely powerful hyphenated technique that was used to identify the organic compounds which were present in the solution [34]. Organic compounds from spent AC and regenerated AC were extracted by anhydrous methanol, and then the organic compounds were analyzed by the GC-MS. Table 2 shows the relative percentages of the chemical composition for spent AC and regenerated AC. Compared with AC, organic compounds on AC were changed before and after regeneration shown in Fig. 5. According to the analysis, there were 11 kinds of organic compounds in spent AC. After regeneration, there were only six kinds of organic compounds on AC, and five kinds of organic compounds were decomposed in the regeneration process. Moreover, the content of organic compounds on regenerated AC was significantly lower than that of the spent AC. The results showed that the organic compounds adsorbed by AC have been decomposed and the pore structure of AC was recovered after regeneration. Therefore, the adsorption performance of AC was also recovered after regeneration.

3.5. Effect of contact time

The effect of contact time on the removal efficiency of Eosin Y varied at the range of 20–80 min. As shown in Fig. 6(A), the removal efficiency of Eosin Y increased with the increase in contact time, and equilibrium was attained after some time. The time required for different concentrations (100 and 140 mg/L) of Eosin Y to reach equilibrium was 60 and 70 min, respectively. The reason behind this trend is that all of the adsorption sites are vacant at the beginning of adsorption, but the adsorption sites are getting occupied

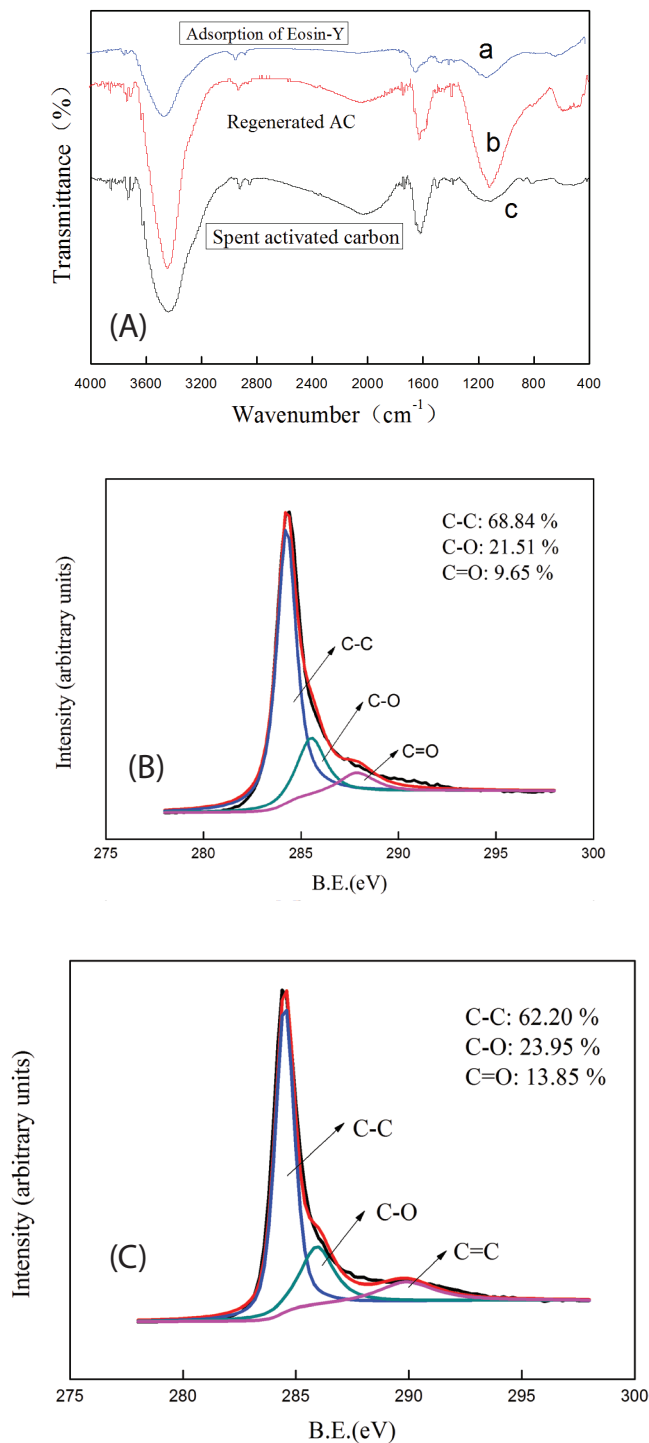


Fig. 4. FTIR of the spent activated carbon, regenerated AC and after adsorption of Eosin Y (A), C 1s XPS of spent activated carbon (B) and C 1s XPS of the regenerated activated carbon (C).

Table 2
Chemical compositions of activated carbon with relative content

Spent activated carbon		Regenerated activated carbon	
Compound	Relative content (%)	Compound	Relative content (%)
2-Pentanone	5.46	2-Pentanone	27.8
Butanoic acid, methyl ester	35.3	Butanoic acid, methyl ester	32.1
3-Pentanone, 2-methyl	2.33	3-Pentanone, 2-methyl	10.04
Butanoic acid, 2-methyl, methyl ester	15.4	Butanoic acid, 2-methyl, methyl ester	23.3
Methyl valerate	4.52	Hexadecanoic acid, methyl ester	3.86
Decane, 2,4,6-trimethyl	0.57	Methyl stearate	2.89
Cyclohexasiloxane, dodecamethyl	1.49		
Cycloheptasiloxane, tetradecamethyl	1.13		
Acetaminophen	32.28		
Hexadecanoic acid, methyl ester	0.99		
Methyl stearate	0.54		

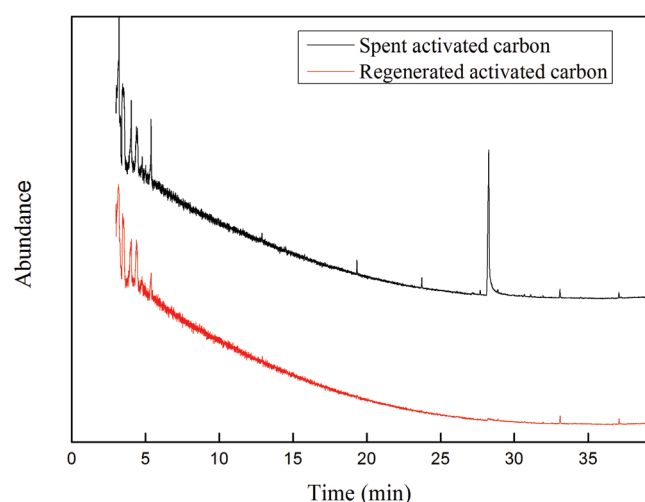


Fig. 5. The GC-MS total ion chromatogram of the spent activated carbon and regenerated activated carbon.

with contact time increase which results in a decrease in the adsorption rate. After a period of time, the adsorption reached the equilibrium, and therefore, the remaining experiments were performed under the equilibrium time at 70 min. Boota et al. [35] and Gupta and Gogate [5] also reported that removal efficiency increased with contact time and reached the equilibrium time in their case was 240 min for Cu(II) removal using citrus reticulata and 20 min for copper removal from wastewater using the activated watermelon based biosorbent.

3.6. Effect of pH

The pH of the dye solution is the second important factor on the removal efficiency of dyes. The effect of pH on removal efficiency of Eosin Y over a range of 2–10 was investigated (Fig. 6(B)). It was observed that removal efficiency of Eosin Y was decreased with increase of pH, and maximum removal is achieved (99.46%) at the pH of 2. Habila et al. [36] studied that

the maximum removal of tartrazine dye onto mixed-spent AC was obtained at a pH of 2. It could be explained that there are a large number of various functional groups on the AC, such as O–H, C=C and C=O. These groups were detected from FTIR results, and it is the main functional groups for adsorption impurities. The occurrence of the double bond was committed to enhancing the interaction between dyes and AC [37]. The reason of this phenomenon is that pH could influence the surface charge of the AC and the degree of ionization. The charge of Eosin Y in the solution is negative. With the increase of pH, the surface of the AC is full of H⁺, so the negative charge Eosin Y is attracted onto AC due to electrostatic interaction. However, the effect of pH on the removal efficiency of Eosin Y is significantly small when the solution pH is from 2 to 6. Thus, the chosen pH of Eosin Y is 6. The remaining experiments were performed under the pH of 6. Gautam et al. [4] also reported a similar conclusion of using AC from the Alligator weed as the adsorbent, and pH effects the removal of tartrazine.

3.7. Effect of temperature

The effect of temperature on the removal efficiency of Eosin Y was investigated among different temperatures of 293, 303 and 313 K (Fig. 6(C)). With an increase in temperature, the removal efficiency of Eosin Y increased. The reason is that the temperature rise can increase the mobility of Eosin Y ion and the rate of diffusion [38]. Besides, the temperature increase also improves the contact opportunity with AC. Based on the thermodynamic studies, the adsorption of Eosin Y with AC was endothermic [39]. Therefore, the removal efficiency of Eosin Y increases with the increase of temperature. Overall, the effect of temperature on the removal rate of Eosin Y was also a decisive factor. In order to facilitate the experiments, the remaining experiments were conducted at room temperature of 30°C [5].

3.8. Effect of initial concentration

The effect of initial concentration on the removal efficiency of Eosin Y has been investigated with initial concentration of 100–180 mg/L (Fig. 6(D)). As shown in Fig. 6(D),

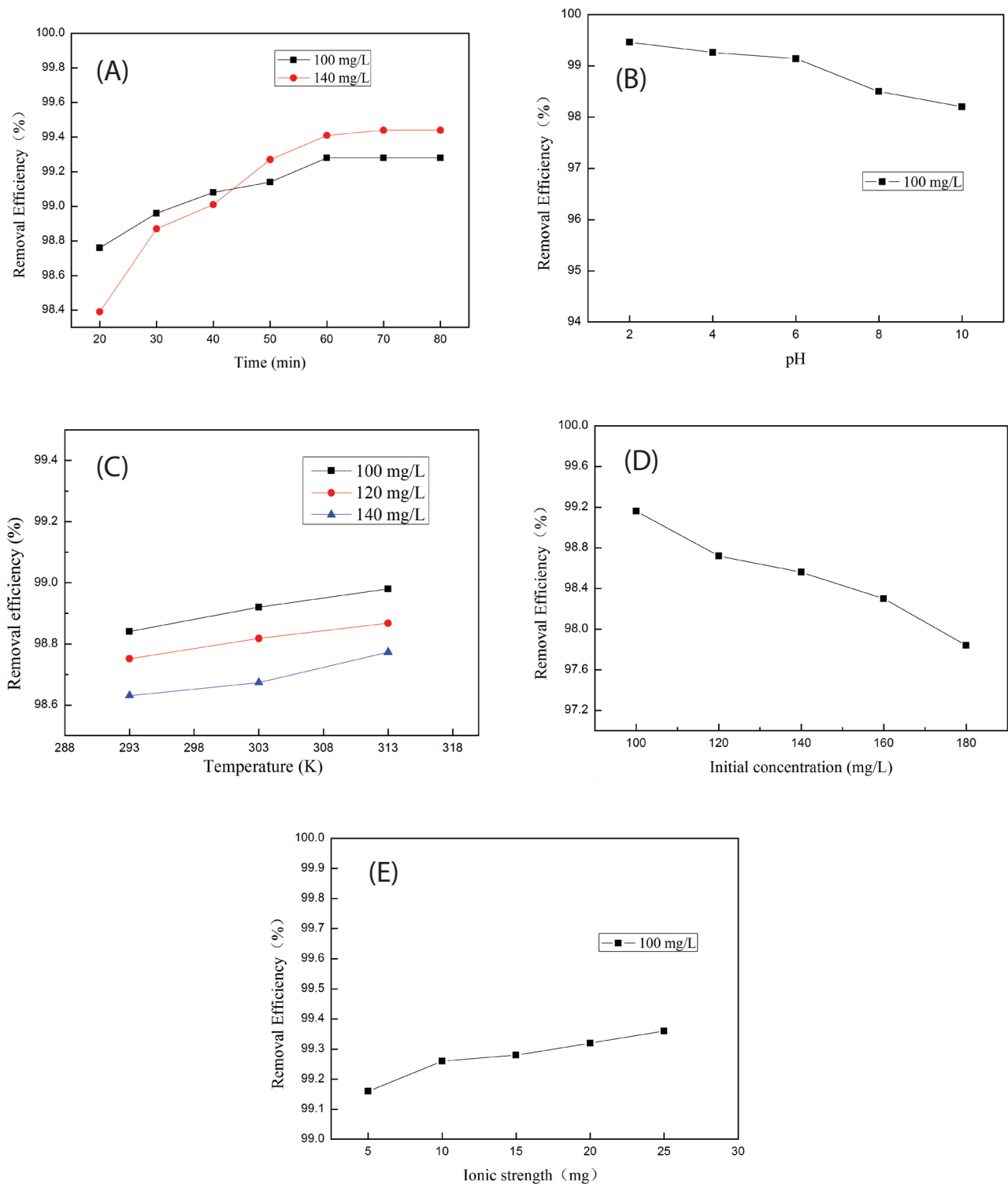


Fig. 6. Effect of contact time (A), pH (B), temperature (C), initial concentration (D) and ionic strength (E) on removal efficiency of Eosin Y.

the removal efficiency of Eosin Y decreased with increase in Eosin Y dye concentration. It can be explained that there was a competition adsorption for AC between the Eosin Y dye and more Eosin Y dye ions compete for limited adsorption

sites at higher concentrations. Therefore, the mass transport and removal efficiency decreased. Ghaedi et al. [40] got the similar results about the effect of initial concentration on the removal of methyl orange.

3.9. Effect of ionic strength

Ionic strength of the dye solution is also a significant parameter for the removal efficiency of Eosin Y. Fig. 6(E) shows that the removal efficiency of Eosin Y increased from 99.16% to 99.36% with the ionic strength increasing from 5 to 25 mg. The ionic strength is changed by adding NaCl. The Eosin Y dye is a water-soluble macromolecule organic matter. Therefore, increasing ionic strength will reduce the adsorbate molecules or ions, which may promote adsorption. The reason is that the adsorbate molecule or ion size becomes smaller, and thus, the adsorbent surface can accommodate more adsorbates and that were also more likely to be adsorbed [41]. On the other hand, the adsorbate can enter a smaller adsorbent pore. The increase of ionic strength may also cause aggregation of surfactant molecule or ion adsorption, and increase of the adsorption capacity.

3.10. Adsorption isotherm

Adsorption isotherm can support us to understand the adsorption behavior better, and obtain more useful information regarding the complex mechanism of interaction between the adsorbate and the adsorbent [42]. In addition, it can help us predict the adsorption capacity of the adsorbent at the fixed temperature for equilibrium. Adsorption experiments were carried out at different initial concentrations and temperatures of 20°C, 30°C and 40°C. In this work, Freundlich and Langmuir isotherm models were adopted to fit the equilibrium data. The adsorption parameters were calculated and summarized in Table 3. According to the adsorption equilibrium data, it fitted the Langmuir model well. Besides, this model is featured with the high correlation coefficient and large adsorption capacity. Therefore, the adsorption process accords with the monolayer adsorption. In other words, the adsorption of Eosin Y could not obey the Freundlich model well. Therefore, the adsorption of Eosin Y based on the monolayer coverage, and the Langmuir isotherm for Eosin Y removal by regenerated AC at different temperatures is shown in Fig. 7.

The adsorption capability of Eosin Y with various adsorbents from the literature is summarized in Table 4. It can be established that the capacity of regenerated AC in this work was higher than that of many adsorbents in Table 4, which indicated that regenerated AC was a kind of potential environmentally friendly adsorbent.

3.11. Adsorption kinetics

It is important to carry out a kinetic analysis for any kind of adsorption process, since it is conducive to determining the applicability of the adsorption process and provides useful information for following adsorption experiments [5]. Furthermore, it can not only describe the adsorption mechanism of AC for Eosin Y but also can indicate the adsorption efficiency of the adsorbent. The adsorption kinetics was analyzed using different models such as pseudo-first-order and pseudo-second-order kinetics and intra-particle diffusion to find the most suitable model based on the value of the linear regression correlation coefficient (R^2). The detailed parameters of models were calculated and shown in Table 5. The correlation coefficients of three models were relatively high. However, pseudo-second-order model has the biggest correlation coefficient, which is close to 1. In addition, for the pseudo-second-order model, the calculated value of Q_e is closest to the actual value Q_0 . Therefore, the pseudo-second-order model is more suitable for the removal efficiency of Eosin Y from AC. This result was consistent with the literature reports that the removal of Eosin Y dyes by synthesis of nano-sized chitosan blended PVA by Anitha et al. [49]. Fig. 8 shows the pseudo-second-order model for the adsorption of Eosin Y at 30°C under various initial concentrations. As shown in Table 5, the values of k_1 and k_2 decreased with the increase of

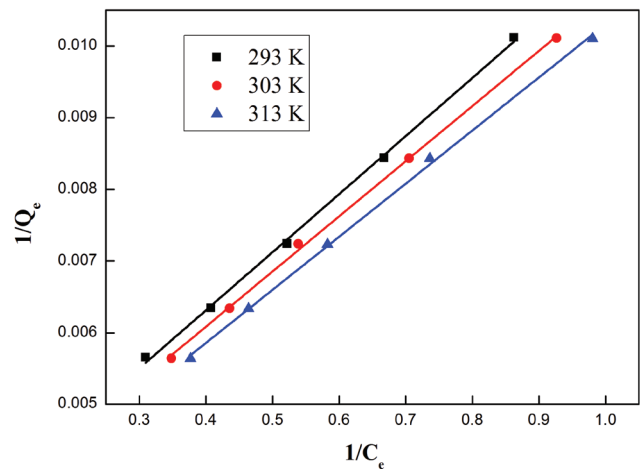


Fig. 7. Langmuir isotherm for Eosin Y removal with regenerated activated carbon.

Table 3
Isotherm constants for Langmuir model and Freundlich model

Isotherm	Equation	Parameters	Adsorbent		
			293 K	303 K	313 K
Langmuir	$\frac{1}{Q_e} = \frac{1}{K_a Q_m C_e} + \frac{1}{Q_m}$	Q_m (mg/g)	324.68	322.58	344.83
		K_a (L/mg)	0.380	0.403	0.391
		R^2	0.998	0.999	0.999
Freundlich	$\log Q_e = \log K_f + \frac{1}{n} \log C_e$	$1/n$	0.6118	0.6484	0.7515
		K_f (L/mg)	89.12	95.50	99.31
		R^2	0.920	0.950	0.959

Table 4
Comparison the maximum monolayer adsorption of Eosin Y onto different adsorbent

Adsorbent	Adsorbate	Q_{\max} (mg/g)	References
Regenerated AC	Eosin Y	344.83	Present work
Conditioned chitosan hydrobeads	Eosin Y	80.84	[43]
Commercial activated carbon	Eosin Y	571.40	[44]
WBTPA-PC	Eosin Y	400	[45]
Jute fiber carbon	Eosin Y	31.489	[46]
Ethylenediamine-modified chitosan	Eosin Y	294.12	[47]
Granular AC	Eosin Y	101.626	[48]
Chitosan/PVA blend	Eosin Y	52.91	[25]

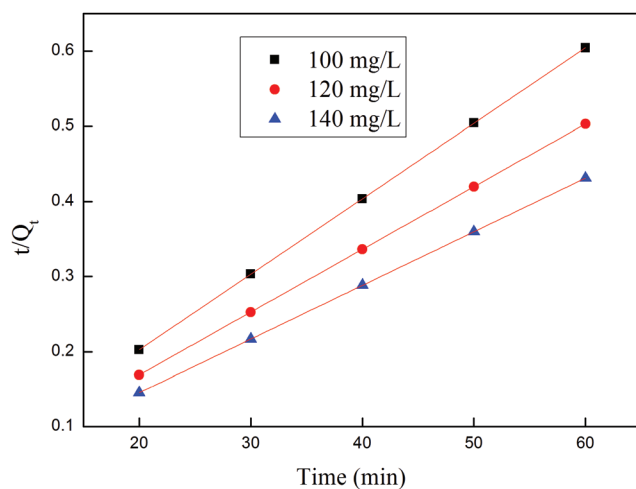


Fig. 8. Non-linear curve fitting of pseudo-second-order.

initial concentration of Eosin Y dyes, while k_3 is opposite. The reason may be that high concentration adsorption sites have higher competition, but the diffusion rate of materials will also be accelerated.

3.12. Thermodynamics

Adsorption thermodynamics was undertaken to investigate the adsorption mechanism of regenerated AC for Eosin Y at different temperatures [50]. Thermodynamic parameters such as the standard free energy (ΔG°), enthalpy (ΔH°) and entropy (ΔS°) were evaluated by previous data and following expressions:

$$K = \frac{Q_e W}{C_e V} \quad (9)$$

$$\Delta G^\circ = -RT \ln K \quad (10)$$

$$\Delta G^\circ = \Delta H^\circ - T \Delta S^\circ \quad (11)$$

$$\ln K = \frac{\Delta S^\circ}{R} - \frac{\Delta H^\circ}{RT} \quad (12)$$

where R (8.314 J/mol K) is the gas constant; T (K) is the temperature; K is the equilibrium constant defined by Q_e and C_e . The values of ΔH° and ΔS° can be calculated by the slopes and intercepts of the plot of $\ln K$ vs. $1/T$ (Fig. 9). The thermodynamic parameter values were shown in Table 6. Negative values of ΔG° for all the temperature indicated the spontaneity of the adsorption process. Positive values of ΔH° reflected the endothermic nature of adsorption, while the positive value of ΔS° was confirmed to be increasing randomly at the solid–liquid interface [4].

3.13. Adsorption mechanism

N_2 adsorption–desorption isotherm curves and FTIR are performed to research the adsorption mechanism. It is well known that the physical adsorption properties of regenerated AC were decided by its physical properties (surface area and pore structure) and chemical adsorption properties of regenerated AC were decided by its surface groups [51]. The BET surface area of regenerated AC is 1,296 m²/g, while the maximum adsorption capacity of regenerated AC on Eosin Y is 344.83 mg/g. While the maximum adsorption capacity of spent AC on Eosin Y is 145 mg/g, and the BET surface area of spent AC is 667.8 m²/g. Compared with spent AC, the BET surface area of regenerated carbon increased by 628 m²/g and the adsorption capacity increased by 199.83 mg/g, which indicated that the Eosin Y adsorption on regenerated carbon is mainly physical adsorption. The FTIR of regenerated carbon and adsorption of Eosin Y are shown in Fig. 4(A). The Fourier spectrum changed after regenerated AC adsorbing the Eosin Y. As shown in Fig. 4(A), the intensity of Eosin Y's adsorption peak is reduced, since the surface functional groups adsorb the Eosin Y and the chemical adsorption that probably happened between AC and Eosin Y.

4. Conclusion

Spent AC was regenerated by microwave heating as an efficient adsorbent to remove Eosin Y from wastewater. The influence of contact time, solution pH, temperature, initial concentration and ionic strength on the adsorption behavior was systematically examined. The equilibrium data were fitted well with Langmuir model, which showed the adsorption based on the monolayer coverage. The maximum adsorption capacity of the Langmuir model was found to be 344.83 mg/g. Adsorption kinetics following the pseudo-second-order model and the rate of the adsorption process was controlled by the diffusion mechanism.

Table 5
Kinetic coefficients of pseudo-first-order and pseudo-second-order kinetic model

Eosin Y concentration (mg/L)	Pseudo-first-order		
	k_1 (min ⁻¹)	Q_e	R^2
100	0.0838	5.665	0.8622
120	0.0769	7.214	0.9408
140	0.0714	8.200	0.9631
Eosin Y concentration (mg/L)	Pseudo-second-order		
	k_2 (g/mg min)	Q_e	R^2
100	0.1713	99.01	0.9999
120	0.08770	119.05	0.9999
140	0.06201	138.89	0.9999
Eosin Y concentration (mg/L)	Intra-particle diffusion		
	k_3 (mg/g)	I	R^2
100	0.1357	98.1911	0.9579
120	0.2677	117.1395	0.9172
140	0.3783	136.2054	0.9369

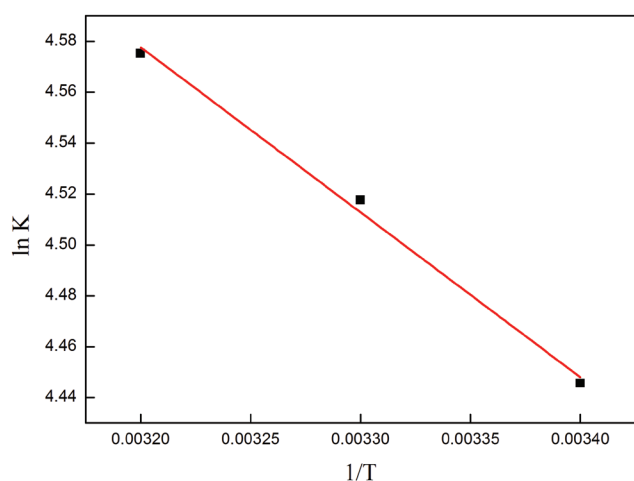


Fig. 9. Van't Hoff plot of Eosin Y in adsorption solution of regenerated AC.

Table 6
Thermodynamic parameter values of regenerated AC adsorption of Eosin Y dye at different temperatures

Temperature (K)	ΔG° (kJ/mol)	ΔH° (kJ/mol)	ΔS° (J/mol K)
293	-10.83	5.38	55.29
303	-11.38		
313	-11.91		

Thermodynamic parameters revealed the endothermic nature of the adsorption process. The results indicated that regenerated AC can be successfully employed as an environmentally friendly and effective adsorbent for the removal of Eosin Y from wastewater.

Acknowledgments

The authors would like to express their gratitude to the Specialized Research Fund for the National Natural Science Foundation of China (51504119), China Scholarship Council (No. 201608740012), Yunnan Applied Basic Research Project (2015FB129) and the Yunnan Provincial Science and Technology Innovation Talents Scheme Technological Leading Talent (2013HA002).

References

- [1] V.D.S. Lacerda, J.B. Lopez-Sotelo, A.C. Guimaraes, Rhodamine B removal with activated carbons obtained from lignocellulosic waste, *J. Environ. Manage.*, 155 (2015) 67–76.
- [2] S. Chen, J. Zhang, C.L. Zhang, Equilibrium and kinetic studies of methyl orange and methyl violet adsorption on activated carbon derived from *Phragmites australis*, *Desalination*, 252 (2010) 149–156.
- [3] E. Daneshvar, A. Vazirzadeh, A. Niazi, M. Kousha, M. Naushad, A. Bhatnagar, Desorption of Methylene blue dye from brown macroalgae: effects of operating parameters, isotherm study and kinetic modeling, *J. Cleaner Prod.*, 152 (2017) 443–453.
- [4] P.K. Gautam, R.K. Gautam, S. Banerjee, Preparation of activated carbon from Alligator weed (*Alternanthera philoxeroides*) and its application for tartrazine removal: isotherm, kinetics and spectroscopic analysis, *J. Environ. Chem. Eng.*, 3 (2015) 2560–2568.
- [5] H. Gupta, P.R. Gogate, Intensified removal of copper from waste water using activated watermelon based biosorbent in the presence of ultrasound, *Ultrason. Sonochem.*, 30 (2016) 113–122.
- [6] D. Charumathi, N. Das, Packed bed column studies for the removal of synthetic dyes from textile wastewater using immobilised dead *C. tropicalis*, *Desalination*, 285 (2012) 22–30.
- [7] S. Banerjee, M.C. Chattopadhyaya, V. Srivastava, Adsorption studies of methylene blue onto activated saw dust: kinetics, equilibrium, and thermodynamic studies, *Environ. Prog. Sustain. Energy*, 33 (2014) 790–799.
- [8] E. Alfaya, O. Iglesias, M. Pazos, Environmental application of an industrial waste as catalyst for the electro-Fenton-like treatment of organic pollutants, *RSC Adv.*, 5 (2015) 14416–14424.
- [9] G.L. Dotto, J.M.N. Santos, I.L. Rodrigues, Adsorption of methylene blue by ultrasonic surface modified chitin, *J. Colloid Interface Sci.*, 446 (2015) 133–140.

- [10] C.T. Weber, G.C. Collazzo, M.A. Mazutti, G.L. Dotto, Removal of hazardous pharmaceutical dyes by adsorption onto papaya seeds, *Water Sci. Technol.*, 70 (2014) 102–107.
- [11] G.C. Collazzo, D.S. Paz, S.L. Jahn, Evaluation of niobium oxide doped with metals in photocatalytic degradation of leather dye, *Lat. Am. Appl. Res.*, 42 (2012) 51–54.
- [12] O. Pezoti Jr., A.L. Cazetta, I.P.A.F. Souza, Adsorption studies of methylene blue onto ZnCl₂-activated carbon produced from buriti shells (*Mauritia flexuosa* L.), *J. Ind. Eng. Chem.*, 20 (2014) 4401–4407.
- [13] A.B. Albadarin, M.N. Collins, M. Naushad, S. Shirazian, G. Walker, C. Mangwandi, Activated lignin-chitosan extruded blends for efficient adsorption of methylene blue, *Chem. Eng. J.*, 307 (2016) 264–272.
- [14] J. Georgin, G.L. Dotto, M.A. Mazutti, Preparation of activated carbon from peanut shell by conventional pyrolysis and microwave irradiation-pyrolysis to remove organic dyes from aqueous solutions, *J. Environ. Chem. Eng.*, 4 (2016) 266–275.
- [15] O.A. Ioannidou, A.A. Zabaniotou, G.G. Stavropoulos, Preparation of activated carbons from agricultural residues for pesticide adsorption, *Chemosphere*, 80 (2010) 1328–1336.
- [16] L. Gao, F.Q. Dong, Q.W. Dai, Coal tar residues based activated carbon: preparation and characterization, *J. Taiwan Inst. Chem. Eng.*, 63 (2016) 166–169.
- [17] P. Paraskeva, D. Kalderis, E. Diamadopoulos, Production of activated carbon from agricultural by-products, *J. Chem. Technol. Biotechnol.*, 83 (2008) 581–592.
- [18] S.H. Yao, J.J. Zhang, D.K. Shen, Removal of Pb(II) from water by the activated carbon modified by nitric acid under microwave heating, *J. Colloid Interface Sci.*, 463 (2016) 118–127.
- [19] S. Cheng, L.B. Zhang, H.Y. Xia, J.H. Peng, J.H. Shu, C.Y. Li, Ultrasound and microwave-assisted preparation of Fe-activated carbon as an effective low-cost adsorbent for dyes wastewater treatment, *RSC Adv.*, 6 (2016) 78936–78946.
- [20] S.C. Ma, Z. Li, J.X. Ma, Influence study of oxygen in the flue gas on physical and chemical properties of activated carbon under microwave irradiation, *J. Environ. Chem. Eng.*, 3 (2015) 1312–1319.
- [21] P. Liao, Z.M. Ismaela, W.B. Zhang, Adsorption of dyes from aqueous solutions by microwave modified bamboo charcoal, *Chem. Eng. J.*, 195–196 (2015) 339–346.
- [22] M. Vadi, Adsorption isotherms of celebrex as non-steroidal anti-inflammation on single-walled carbon nanotubes, *Int. J. Phys. Sci.*, 7 (2012) 1215–1218.
- [23] J. Yang, M. Yu, W. Chen, Adsorption of hexavalent chromium from aqueous solution by activated carbon prepared from longan seed: kinetics, equilibrium and thermodynamics, *J. Ind. Eng. Chem.*, 21 (2015) 414–422.
- [24] H.X. Zhang, Z.W. Niu, Z. Liu, W.S. Wu, Equilibrium, kinetic and thermodynamic studies of adsorption of Th(IV) from aqueous solution onto kaolin, *J. Radioanal. Nucl. Chem.*, 303 (2015) 87–97.
- [25] H.Y. Shan, Review of second-order models for adsorption systems, *J. Hazard. Mater.*, 136 (2006) 681–689.
- [26] S.K. Behera, J.H. Kim, X. Guo, H.S. Park, Adsorption equilibrium and kinetics of polyvinyl alcohol from aqueous solution on powdered activated carbon, *J. Hazard. Mater.*, 153 (2008) 1207–1214.
- [27] N. Saeidi, M. Parvini, Z. Niavarani, High surface area and mesoporous graphene/activated carbon composite for adsorption of Pb(II) from wastewater, *J. Environ. Chem. Eng.*, 3 (2015) 2697–2706.
- [28] O. Pezoti, A.L. Cazetta, K.C. Bedin, NaOH-activated carbon of high surface area produced from guava seeds as a high-efficiency adsorbent for amoxicillin removal: kinetic, isotherm and thermodynamic studies, *Chem. Eng. J.*, 288 (2016) 778–788.
- [29] N.M. Nor, M.F.F. Sukri, A.R. Mohamed, Development of high porosity structures of activated carbon via microwave-assisted regeneration for H₂S removal, *J. Environ. Chem. Eng.*, 4 (2016) 4839–4845.
- [30] M. Ahmaruzzaman, V.K. Gupta, Rice husk and its ash as low-cost adsorbents in water and wastewater treatment, *Ind. Eng. Chem. Res.*, 50 (2011) 13589–13613.
- [31] X.C. Lu, J.C. Jiang, K. Sun, Influence of the pore structure and surface chemical properties of activated carbon on the adsorption of mercury from aqueous solutions, *Mar. Pollut. Bull.*, 78 (2014) 69–76.
- [32] C.T. Weber, E.L. Foletto, L. Meili, Removal of tannery dye from aqueous solution using papaya seed as an efficient natural biosorbent, *Water Air Soil Pollut.*, 224 (2013) 1427–1433.
- [33] F. Li, J.W. Zhang, X.L. Wang, X-ray photoelectron spectroscopy study of Schottky junctions based on oxygen-/fluorine-terminated (100) diamond, *Diamond Relat. Mater.*, 63 (2016) 180–185.
- [34] B.B. Krishna, B. Biswas, P. Ohri, J. Kumar, T. Bhaskar, Pyrolysis of *Cedrus deodara* saw mill shavings in hydrogen and nitrogen atmosphere for the production of bio-oil, *Renew. Energy*, 98 (2016) 238–244.
- [35] R. Boota, H.N. Bhatti, M.A. Hanif, Removal of Cu(II) and Zn(II) using lignocellulosic fiber derived from *Citrus reticulata* (Kinnow) waste biomass, *Sep. Sci. Technol.*, 44 (2009) 4000–4022.
- [36] M.A. Habila, Z.A. AlOthman, R. Ali, Removal of tartrazine dye onto mixed-waste activated carbon: kinetic and thermodynamic studies, *CLEAN-Soil Air Water*, 42 (2014) 1824–1831.
- [37] P. Pengthamkeerati, T. Satapanajaru, O. Singchan, Sorption of reactive dye from aqueous solution on biomass, *J. Hazard. Mater.*, 153 (2008) 1149–1156.
- [38] O. Hamdaoui, M. Chiha, E. Naffrechoux, Ultrasound-assisted removal of malachite green from aqueous solution by dead pine needles, *Ultrason. Sonochem.*, 15 (2008) 799–807.
- [39] T. Karthikeyan, S. Rajgopal, L.R. Miranda, Chromium(VI) adsorption from aqueous solution by *Hevea Brasiliensis* sawdust activated carbon, *J. Hazard. Mater.*, 124 (2005) 192–199.
- [40] M. Ghaedi, A.M. Ghaedi, B. Mirtamizdoust, Simple and facile sonochemical synthesis of lead oxide nanoparticles loaded activated carbon and its application for methyl orange removal from aqueous phase, *J. Mol. Liq.*, 213 (2016) 48–57.
- [41] Z.J. Wu, H.N. Liu, H.F. Zhang, Progress in the study of the effect of ionic strength on adsorption, *Environ. Chem.*, 29 (2010) 997–1003.
- [42] D.S. Paz, A. Baiotto, M. Schwaab, Use of papaya seeds as a biosorbent of methylene blue from aqueous solution, *Water Sci. Technol.*, 68 (2013) 441–447.
- [43] S. Chatterjee, S. Chatterjee, B.P. Chatterjee, Adsorption of a model anionic dye, eosin Y, from aqueous solution by chitosan hydrobeads, *J. Colloid Interface Sci.*, 288 (2005) 30–35.
- [44] M.K. Purkait, S. DasGupta, S. De, Adsorption of eosin dye on activated carbon and its surfactant based desorption, *J. Environ. Manage.*, 76 (2005) 135–142.
- [45] L. Borah, M. Goswami, P. Phukan, Adsorption of methylene blue and eosin yellow using porous carbon prepared from tea waste: adsorption equilibrium, kinetics and thermodynamics study, *J. Environ. Chem. Eng.*, 3 (2015) 1018–1028.
- [46] K. Porkodi, K.V. Kumar, Equilibrium, kinetics and mechanism modeling and simulation of basic and acid dyes sorption onto jute fiber carbon: eosin yellow, malachite green and crystal violet single component systems, *J. Hazard. Mater.*, 143 (2007) 311–327.
- [47] X.Y. Huang, J.P. Bin, H.T. Bu, Removal of anionic dye eosin Y from aqueous solution using ethylenediamine modified chitosan, *Carbohydr. Polym.*, 84 (2011) 1350–1356.
- [48] U. Iriarte-Velasco, N. Chimeno-Alanís, M.P. González-Marcos, Relationship between thermodynamic data and adsorption/desorption performance of acid and basic dyes onto activated carbons, *J. Chem. Eng. Data*, 56 (2011) 2100–2109.
- [49] T. Anitha, P.S. Kumar, K.S. Kumar, Synthesis of nano-sized chitosan blended polyvinyl alcohol for the removal of Eosin Yellow dye from aqueous solution, *J. Water Process Eng.*, 13 (2016) 127–136.
- [50] Y. Bulut, H. Aydın, A kinetics and thermodynamics study of methylene blue adsorption on wheat shells, *Desalination*, 194 (2006) 259–267.
- [51] L.B. Zhang, Y.H. Liu, S.X. Wang, B.G. Liu, J.H. Peng, Selective removal of cationic dyes from aqueous solutions by an activated carbon-based multicarboxyl adsorbent, *RSC Adv.*, 5 (2015) 99618–99626.